JOURNAL OF MATERIALS SCIENCE 29 (1994) 4592–4603

An investigation on the bearing test procedure for fibre-reinforced aluminium laminates

H. F. WU*, L. L. WU
Alcoa Technical Center, Alcoa Center, PA 15069, USA
W. J. SLAGTER
Delft University of Technology, Delft, The Netherlands

Excellent fatigue, static strength and damage tolerance characteristics together with low density make fibre-reinforced aluminium laminates a prime candidate sheet material for application in fatigue- and fracture-critical aircraft structures. Their use requires that mechanical property design allowables be established for incorporation in design handbooks (e.g. MIL-HDBK-5). An experimental programme based on statistical design was conducted to establish a meaningful test procedure for determination of fibre–metal laminate bearing strength design allowables. The test procedures investigated are the pin-type bearing test method (ASTM E-238) and the bolt-type bearing test method, a modified method based on the procedure for bearing strength determinations in plastics (ASTM D-953). Results are presented from an experimental programme which measured the bearing strengths of two grades of S-2 glass-based and one grade of aramid-based aluminium laminates. The influences of lateral constraint and ply orientation on bearing strength and failure mode are shown. The bolt-type bearing test method, which combines the attributes of the two aforementioned methods, is recommended. The study also showed that the bearing properties for edge distance ratio $e/D = 2$ can be predicted by correlation with the aluminium volume fraction in fibre-reinforced aluminium laminates. In addition, diagrams of joint structural efficiency, shown to be comparable to those of aluminium alloy sheets, have been established.

1. Introduction

Fibre–metal laminates are arrangements of thin, high-strength aluminium alloy sheets bonded to alternating plies of fibre-reinforced epoxy adhesive. They represent a new class of aerospace sheet materials that combine the best features of pure composites and metals [1–12]. Fibre–metal laminates offer the same magnitude of weight reduction [13–15] and structural performance as graphite–epoxy composites while retaining the familiar design, ease of manufacture and support characteristics of aluminium. Fibre–metal laminates provide the opportunity for distinctive advances in structures at a much lower risk than graphite–epoxy composites. In addition, fibre–metal laminates also exhibit good thermal stability in cryogenic and elevated-temperature environments [16–18].

At present, fibre–metal laminates are the only available structural sheet materials that combine the fatigue insensitivity of composites with the damage-tolerant capability of metals. Their ability to impede and arrest crack growth makes them promising candidates as fuselage materials in next-generation civil transport aircraft. Development of fibre–metal laminates to meet the stringent demands of fuselage applications could revolutionize airframe construction by providing aircraft designers with a robust portfolio of high performance, engineered materials. The need for such materials is graphically demonstrated by current problems and safety concerns with our "ageing aircraft" fleet.

First- and second-generation laminate forms given in Tables I and II have been standardized as product benchmarks. Each product benchmark employs thin, high-strength (7475 or 2024 type) aluminium alloy sheets alternating with layers of adhesive-impregnated fibres. A generic schematic representation of a 3/2 lay-up (i.e. three layers aluminium alloy sheet and two layers prepreg) of fibre–metal laminates is shown in Fig. 1. To date, most experience has been obtained on laminate products employing 0.012 in. (0.30 mm) gauge aluminium sheet; however, 0.0085 in. (0.22 mm) and 0.016 in. (0.41 mm) sheet gauges are also available for use. The first-generation ARALL laminates employ aramid fibres in a uniaxial configuration, while the second-generation GLARE laminates employ

Present address: Owens-Corning Science and Technology Center, Ohio 43023, USA.

0022–2461

TABLE I Standardized first-generation laminate product forms

Product variant	Description
ARALL 1	Alloy: 7475-T6, bonding surfaces anodized and primed Prepreg: 250 °F cure epoxy adhesive with unidirectional aramid fibres Post-cure: 0.4% permanent stretch
ARALL 2	Alloy: 2024-T3, bonding surfaces anodized and primed Prepreg: 250 °F cure epoxy adhesive with unidirectional aramid fibres
ARALL 3	Alloy: 7475-T76, bonding surfaces anodized and primed Prepreg: 250 °F cure epoxy adhesive with unidirectional aramid fibres Post-cure: 0.4% peramanent stretch
ARALL 4	Alloy: 2024-T8, bonding surfaces anodized and primed Prepreg: 350 °F cure epoxy adhesive with unidirectional aramid fibres

TABLE II Standardized second-generation laminate product forms

Product variant	Description
GLARE 1	Alloy: 7475-T76, bonding surfaces anodized and primed Prepreg: 250 °F cure epoxy adhesive with unidirectional glass fibres Post-cure: 0.5% permanent stretch
GLARE 2	Alloy: 2024-T3, bonding surfaces anodized and primed Prepreg: 250 °F cure epoxy adhesive with unidirectional glass fibres
GLARE 3	Alloy: 2024-T3, bonding surfaces anodized and primed Prepreg: 250 °F cure epoxy adhesive with cross-ply glass fibres 50% fibres in longitudinal aluminium sheet direction 50% fibres in long-transverse aluminium sheet direction
GLARE 4	Alloy: 2024-T3, bonding surfaces anodized and primed Prepreg: 250 °F cure epoxy adhesive with cross-ply glass fibres 70% fibres in longitudinal aluminium sheet direction 30% fibres in long-transverse aluminium sheet direction

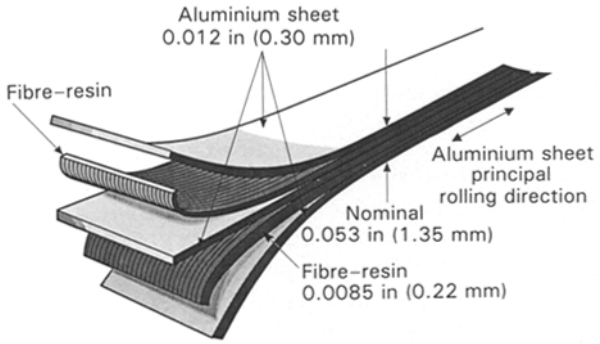

Figure 1 Fibre–metal structural laminates (typical 3/2 lay-up shown). Standard constituent materials: aluminium sheet alloy 2024 or 7475, aramid or glass fibre, unidirectional or cross-ply prepreg.

glass fibres which may be in either a uniaxial or an orthogonal cross-ply arrangement. Cross-ply fibre systems have been explored with some success and are generally better suited to biaxial load situations typical of aircraft fuselage skins.

A design prerequisite for the introduction into service of fibre–metal laminates is the development and presentation of minimum mechanical property allowables consistent with the format of the Military Standardization Handbook, MIL-HDBK-5 [19]. This handbook is the primary source of design mechanical properties for metallic structural materials, and its use is mandated in the design of aerospace vehicles controlled or procured by Department of Defense (DoD) agencies, the Federal Aviation Administration (FAA) and the National Aeronautics and Space Administration (NASA). Bearing strength is one of the important static property allowables in the statistical basis format required for MIL-HDBK-5 incorporation.

Due to the nature of the anisotropy in fibre–metal laminates, characterizing the bearing strength in these hybrid materials is more complex than in conventional aluminium alloys. In order to fully understand bearing mechanical behaviour, developing a meaningful test procedure is mandatory. Based upon our experience with an ARALL 3 laminate MIL-HDBK-5 design allowable programme and a literature search, we found that the bearing strength depends on some relevant parameters. These include

(i) material parameters: fibre-type and form (unidirectional or bi-axial), resin type, fibre orientation, laminate stacking sequence, fibre volume fraction and fibre surface treatment;

(ii) *fastener parameters*: fastener type (screw, bolt or rivet), fastener size, clamping force, washer size, and hole size and tolerance; and

(iii) *design parameters*: joint type (single lap or single cover butt), laminate thickness and tolerance, geometry (pitch, edge distance, width, hole pattern), load direction, loading rate, static or dynamic load, and failure criteria.

This test evaluation programme will focus on the study of some of the key factors that influence the bearing mechanical behaviour and will optimize the relevant parameters affecting the bearing strength in fibre–metal laminates. The purpose of this research is

not only to develop a meaningful bearing test procedure but also to help designers optimize the edge distance, laminate width and pin-hole size (or laminate thickness). This will assist designers in developing full bearing strength for joints in structures and in preventing the mechanical fasteners from failing in shear, tension or cleavage modes during their operation.

2. Failure modes

Recently Wu *et al.* [20, 21] presented the S-basis minimum strength properties for ARALL 3 laminates from their MIL-HDBK-5 programme. In their design allowable programme, a large number of static tests were conducted. In the bearing testing, they found that the bearing ultimate strength was strongly dependent on the failure modes. The failure mechanisms of ARALL laminates showed typical metal-like failure modes such as those shown in Fig. 2. However, their failure mechanisms are more complex and different due to delamination buckling and depend on many factors such as fibre–matrix type, fibre orientation, laminate stacking sequence, fibre volume fraction, fibre surface treatment, clamping force, hole size and tolerance, laminate thickness, geometry (edge distance, width effect) and test procedure. The effects of these parameters on bearing test results have been described in the literature [22–28].

2.1. Tension failure

As with conventional materials, the tensile load required for a laminate to fail through a section with holes (net section) is less than at a section in which there are no holes (gross section). The stresses at these sections, at failure, are given respectively by

$$\sigma_N = \frac{P}{(W - D)t} \tag{1}$$

and

$$\sigma_G = \frac{P}{Wt} \tag{2}$$

where P is the failing load of the laminate, W the laminate width at the gross section, D the pin-hole diameter and t the laminate thickness. The tensile strength efficiency achieved at these sections, expressed in the form of average net and gross stress concentrations, is given by

$$k_N = \sigma_\infty/\sigma_N \tag{3}$$

and

$$k_G = \sigma_\infty/\sigma_G \tag{4}$$

where σ_∞ is the theoretical ultimate tensile strength of a plain laminate.

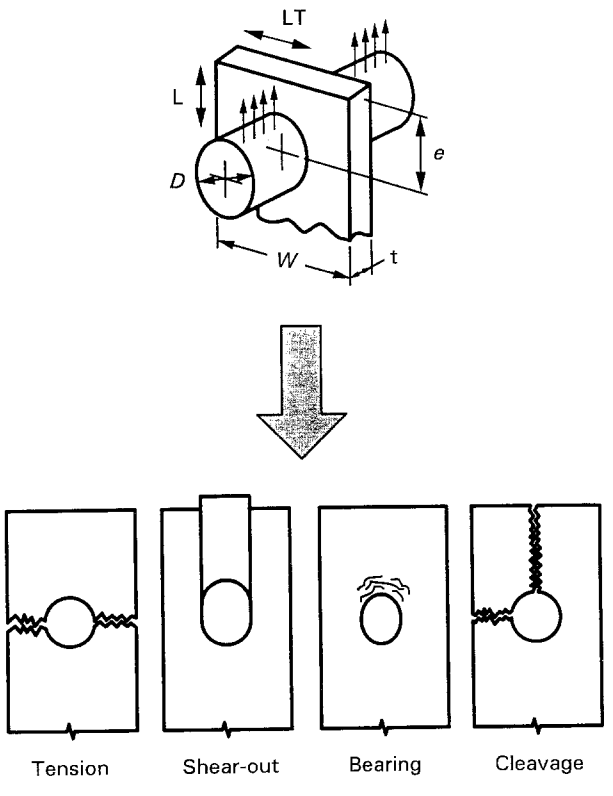

Figure 2 Typical failure modes of bearing test for ARALL laminates.

2.2. Shear failure

The shear strength normally quoted for fibre–metal laminates is the interlaminar shear strength obtained using the short-beam shear test. The in-plane shear strength can be measured using the Iosipescu shear test [29, 30]. The shear strength, as for conventional isotropic materials, is given as

$$\tau = P/2et \tag{5}$$

where e is the edge distance (parallel to the load) between the hole centre and the free edge.

2.3. Bearing failure

Bearing of a pin in a hole gives rise to compressive stresses around the loaded half of the circumference of the hole. For practical purposes the bearing strength of hybrid laminates, like that of a conventional material, is usually expressed as the average projected stress acting uniformly over the cross-sectional area of the hole, so that

$$\sigma_b = P/Dt \tag{6}$$

In the previous work performed by Wu *et al.* [20, 21], all bearing tests in the MIL-HDBK-5 ARALL 3 laminate design allowable programme were conducted in accordance with the ASTM E-238 [31] test procedure, which is applicable to conventional aluminium alloy products as described in MIL-HDBK-5. Bearing strengths in both the longitudinal (L) and the long-transverse (LT) directions with e/D ratios of 1.5 and 2.0 were used in this test programme. Here, L is also parallel to aluminium alloy sheet principal rolling direction and LT is perpendicular to the principal rolling direction of aluminium alloy sheet. Four types of lay-up of ARALL 3 laminates (2/1, 3/2, 4/3 and 5/4) were selected. Six tests per test direction per lay-up were performed. Table III summarizes the failure modes of the bearing tests in the MIL-HDBK-5 programme.

TABLE III Summary of ARALL 3 laminate bearing failure mode distribution

Lay-up	$e/D = 1.5$						$e/D = 2.0$					
	L[a]			LT[a]			L			LT		
	S[b]	B[b]	C[b]	S	B	C	S	B	C	S	B	C
2/1	24				24			24			24	
3/2	24				24			24			24	
4/3	24				24			24			24	
5/4			24		24			24			24	

[a]Test direction L = longitudinal, LT = long-transverse.
[b]Failure mode S = shear-out, B = bearing, C = cleavage (see Fig. 2).

As the width of the specimen decreases, there is a point where the mode of failure changes from bearing to net section tension, i.e. the specimen fails across the width at the net section, with cracks originating from the hole boundary. As the edge distance decreases, the bearing failure mode changes to one of shear-out. In this design allowable programme the results show that a total number of 96 bearing tests in the longitudinal direction having $e/D = 1.5$ failed in either shear-out or cleavage mode. This indicates that the full bearing strength was not totally achieved when the edge distance ratio equalled 1.5 in the longitudinal test specimen. The remaining 288 tests failed in the bearing mode. However, a delamination buckling bearing failure commonly occurred around the pin hole for ARALL laminates. The absence of lateral constraint in this test set-up allows this type of failure which has been analysed and discussed extensively elsewhere [32]. Previous work [27, 28, 32] has also demonstrated that lateral constraint substantially enhances the bearing strength performance of laminates. In contrast, aluminium alloy sheet usually showed more uniform deformation of bearing failure around the pin hole. This suggests that an out-of-plane buckling failure of ARALL laminates has occurred during the test. The anisotropic nature of fibres may also induce a high magnitude of stress concentration around the pin hole. Several hypotheses can be drawn from various failure mode observations:

1. High stress concentration magnitudes occur around the pin hole due to the nature of the anisotropy of the hybrid laminates.
2. Full bearing strength is not developed with current parameters of e/D, W/D and D/t ratios (geometry effect).
3. Delamination buckling is a typical bearing failure mode if lateral constraint is not provided.
4. Premature bearing failure happened because of lacking lateral constraint during the testing.

The present experimental programme was directed toward addressing these concerns and hypotheses.

3. Experimental procedure

3.1. Test variables

The bearing strength and the failure modes of fibre-reinforced aluminium laminates depend on four geometric variables: the edge distance, the width, the hole diameter and the laminate thickness. Another important variable is whether the testing procedure is used with or without lateral constraint. A test matrix of bearing strength characterization for ARALL and GLARE laminates by the e/D, W/D, and D/t effects is described in Table IV (for details see Wu [33]). Two test procedures, the pin-type bearing [31] and the bolt-type bearing [34] test methods, were investigated in this programme. Fig. 3 shows the details of these two types of bearing test method. The pin-type bearing test procedure is characterized by the lack of lateral constraint, in contrast to the bolt-type bearing test procedure which can provide lateral constraint. The bearing ultimate strength obtained from the pin-type testing procedure (ASTM E-238) is calculated by dividing the maximum load carried by the specimen by the bearing area, while the bearing ultimate strength obtained from the bolt-type testing procedure (ASTM D-953) is defined by the maximum load occurring before a 4% total deflection of the original bolt hole, divided by the

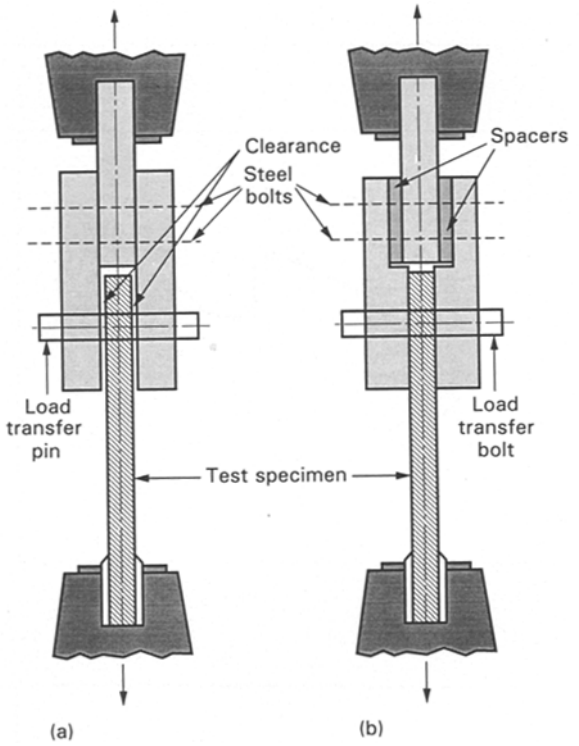

Figure 3 Schematic representation of bearing testing procedures: (a) pin-type bearing without lateral constraint (ASTM E-238), (b) bolt-type bearing providing lateral constraint ASTM D-953).

TABLE IV Test matrix of bearing strength characterization for fibre–metal laminates

	Laminate		
	ARALL 2	GLARE 2	GLARE 3
Metal volume fraction (%)	67.90	64.29	64.29
Test direction	L, LT	L, LT	L
e/D (fixed $W/D = 6$)	1.5, 2, 3, 5	1.5, 2, 3, 5	1.5, 2, 3, 5
W/D (fixed $e/D = 3$)	2, 4, 6, 8	2, 4, 6, 8	2, 4, 6, 8
D/t(fixed $e/D = 3$ and $W/D = 6$ with lateral constraint)	–	3 layers thickness: 2/1, $V_f^{AL} = 70.59\%$ 3/2, $V_f^{AL} = 64.29\%$ 5/4, $V_f^{AL} = 60.00\%$ Three hole sizes: 4, 6.35 and 8 mm	–
With lateral constraint (modified ASTM D-953)	No	Yes	Yes
No lateral constraint (ASTM E-238)	Yes	Yes	No

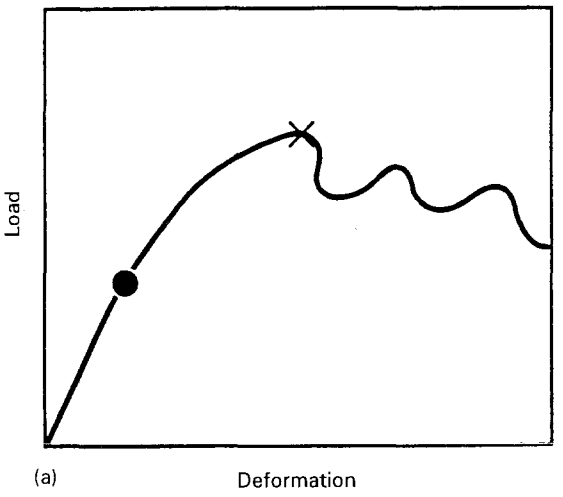

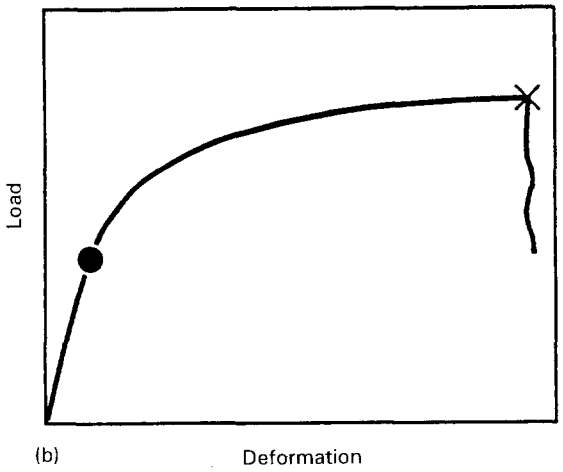

Figure 4 Typical load–deformation curves using (a) pin-type, (b) bolt-type bearing test set-ups. (×) ultimate, (●) proportional limit.

bearing area. Typical load–deflection curves using the pin-type and bolt-type bearing test procedures are shown in Fig. 4.

3.2. Statistical design

Two randomizations were involved in carrying out these statistically designed experiments [33]. The first

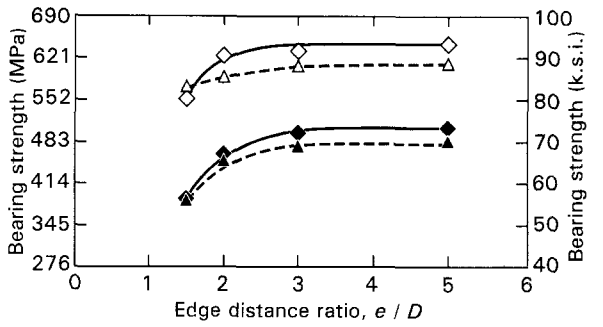

Figure 5 4/3 ARALL 2 laminate pin-type bearing: variation of ultimate strength (BUS) and yield strength (BYS) with e/D ratio. Longitudinal: ◇ BUS, (△) BYS; transverse: (◆) BUS, (▲) BYS. 1 ksi = 6.895 MPa.

was the random assignment of the treatment variables to the specimens cut from each panel. This was done to guard against systematic variations in the properties of the material with position on the panel. The second randomization involved testing the samples in a random time order. This guarded against a systematic drift in the testing system with time. In this experimental programme quadruplicate tests were performed in both longitudinal and LT directions using two different test procedures. Data plotted in the following figures represent an average value from four test data.

4. Results and discussion

4.1. Effect of edge distance

As the edge distance decreases, the mode of failure changes from bearing to shear-out. Tests varying the e/D ratio between 1.5, 2, 3 and 5 were studied on ARALL 2, GLARE 2, and GLARE 3 laminates. The test results the plotted in Figs 5 to 7. In these figures, the transition region of bearing strength of ARALL or GLARE laminates had been developed when $e/D \geq 3$. The e/D effect is shown to be independent of test method. In the tests, the bolt-type bearing test method provided lateral side restraint to reduce stress concentration around the pin hole. This caused the stresses to be distributed more uniformly over a larger area than in a pin-type loaded specimen, resulting in a higher bearing strength.

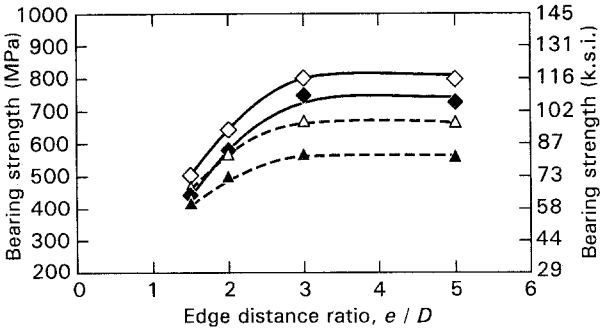

Figure 6 3/2 GLARE 2 laminate bolt-type bearing: variation of ultimate and yield strength with e/D ratio. Longitudinal: ◇ BUS, (△) BYS; transverse: (◆) BUS, (▲) BYS. 1 ksi = 6.895 MPa.

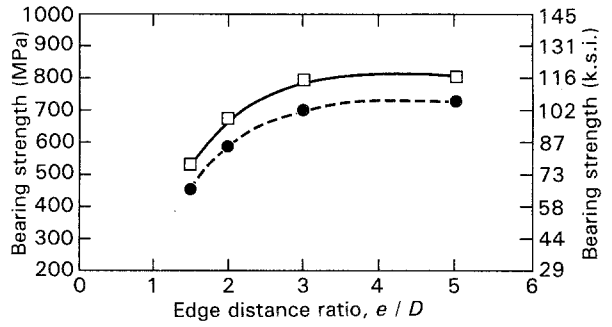

Figure 7 3/2 GLARE 3 laminate bolt-type longitudinal bearing: variation of (□) ultimate and (●) yield strength with e/D ratio. 1 ksi = 6.895 MPa.

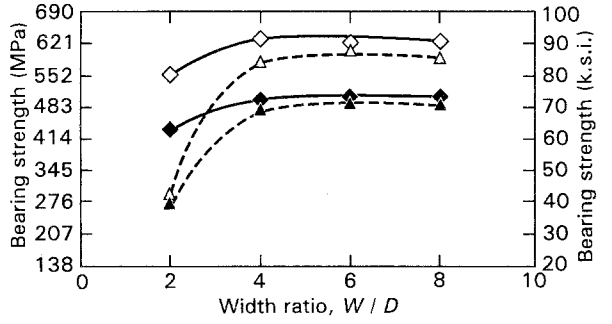

Figure 8 4/3 ARALL 2 laminate pin-type bearing: variation of ultimate and yield strength with W/D ratio. Longitudinal: (◇) BUS, (△) BYS; transverse: (◆) BUS, (▲) BYS. 1 ksi = 6.895 MPa.

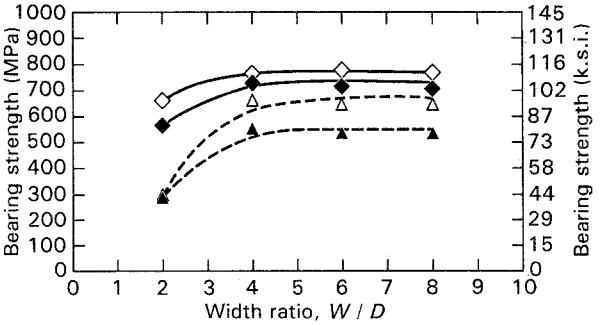

Figure 9 3/2 GLARE 2 laminate bolt-type bearing: variation of ultimate and yield strength with W/D ratio. Longitudinal: (◇) BUS, (△) BYS; transverse: (◆) BUS, (▲) BYS. 1 ksi = 6.895 MPa.

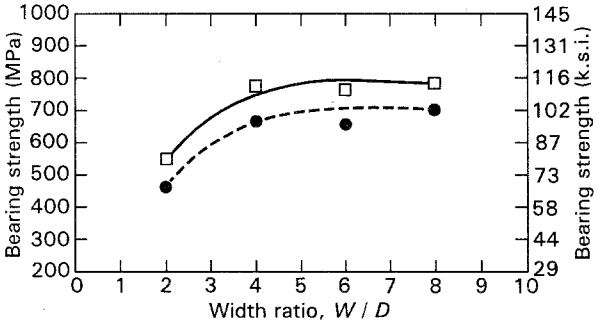

Figure 10 3/2 GLARE 3 laminate bolt-type longitudinal bearing: variation of (□) ultimate and (●) yield strength with W/D ratio. 1 ksi = 6.895 MPa.

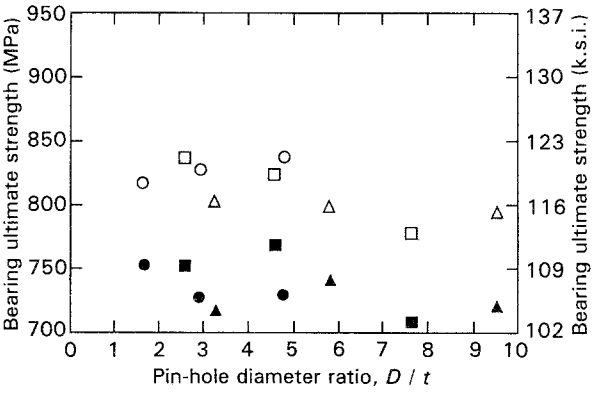

Figure 11 Variation of longitudinal bearing ultimate and yield strengths of 3/2 GLARE 2 laminates with D/t ratio (finger-tight bolt); t = 0.84, 1.38 or 2.47 mm. D = 4 mm: (○) BUS, (●) BYS. D = 6.35 mm: (□) BUS, (■) BYS. D = 8 mm: (△) BUS, (▲). BYS. 1 ksi = 6.895 MPa.

4.2. Effect of width

As the width of the specimen decreases, there is a point where the mode of failure changes from bearing to net-section tension. Tests varying the W/D ratio between 2, 4, 6 and 8 were investigated on ARALL and GLARE laminates. The test results are presented in Figs 8 to 10. It is important to note the gradual asymptotic behaviour of the curves of ARALL and GLARE laminates, revealing a strong influence of the width on the bearing failure load. In the figures, the transition region of bearing strength occurs when $W/D \geq 4$. A D/W value of about 0.25 thus provides optimum joint structural efficiency, which agrees with Hart-Smith's [35] interpretation of bolted joint data in fibrous materials.

4.3. Effect of thickness

An effect of thickness was found if the ratio D/t was examined. In Figs 11 and 12 it is clear that the bearing ultimate strength increases with decreasing D/t for the case of finger-tight bolt-type bearing tests on GLARE 2 laminates. From the current chosen range of holes of 4–8 mm diameter in these two figures, the effect of the pin diameter on bearing strength in the longitudinal direction seems to be more pronounced than in the LT direction. However, the effect of the pin diameter on bearing strength in the LT direction shows insignificant differences when $D/t \geq 3$. In reality, when we attempt to avoid the influence of aluminium volume fraction (by considering a single lay-up), the effect is rather small (even $< 5\%$). Collings [26] and Godwin

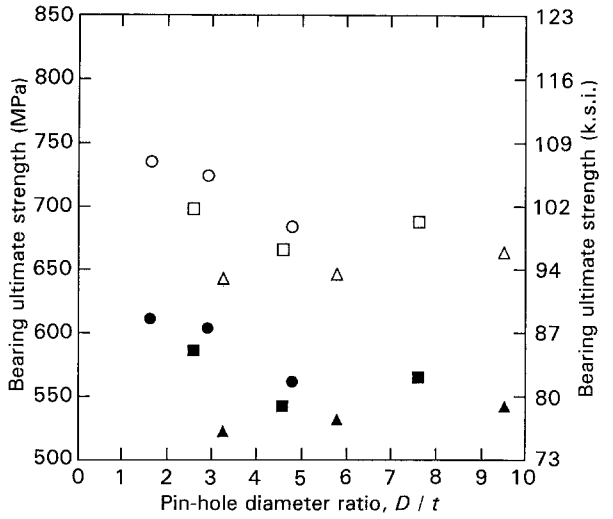

Figure 12 Variation of long-transverse bearing ultimate and yield strengths of 3/2 GLARE 2 laminates with D/t ratio (finger-tight bolt); t = 0.84, 1.38 or 2.47 mm. D = 4 mm: (○) BUS, (●) BYS. D = 6.35 mm: (□) BUS, (■) BYS. D = 8 mm: (△) BUS, (▲) BYS. 1 ksi = 6.895 MPa.

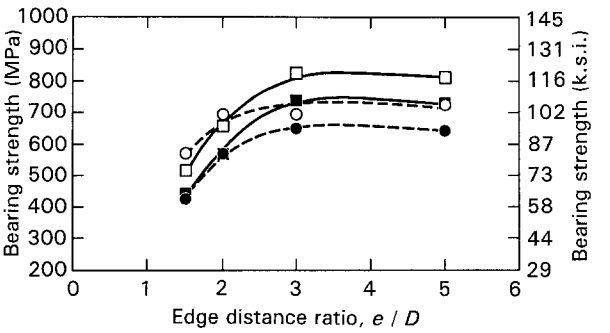

Figure 13 Comparison of longitudinal bearing ultimate and yield strengths of 3/2 GLARE 2 laminates versus e/D ratio using bolt-type and pin-type test fixtures. Bolt type: (□) BUS, (■) BYS; pin type: (○) BUS, (●) BYS.

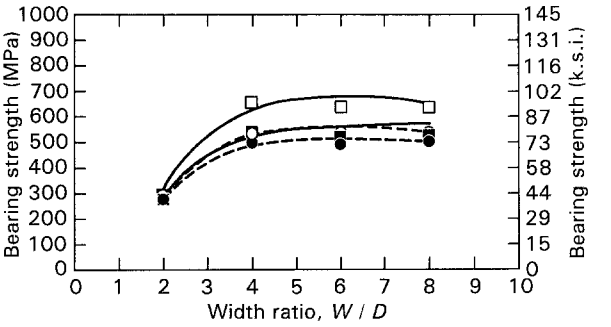

Figure 14 Comparison of long-transverse bearing ultimate and yield strengths of 3/2 GLARE 2 laminates versus W/D ratio using bolt-type and pin-type test fixtures. Bolt type: (□) BUS, (■) BYS; pin type: (○) BUS, (●) BYS.

and Matthews [22] presented similar results for carbon–epoxy composites and other materials, but Collings showed that for high lateral pressure values, the effects of D/t almost disappear.

4.4. Effect of lateral constraint

Studies by Stockdale and Matthews [27] for glass fibre-reinforced plastics and by Eriksson [28] for graphite–epoxy laminates have shown a significant influence of lateral constraint in the bearing tests. A finger-tight pressure was applied to the bolt-type bearing test fixture. This type of side-restraint bearing loading provided a sufficient lateral constraint on the laminate to control the delamination buckling mode. The ultimate load is therefore expected to increase since the easiest failure modes are suppressed. However, the failure mode of the pin-type bearing specimens showed the damage to be localized around the loaded half of the hole, and delamination buckling was easily observed. Figs 13 and 14 show a comparison of bearing strength variation with e/D and W/D ratios using these two types of test fixture, respectively. The results show that the bolt-type test method yields at least a 20% increase in bearing strength over that of the pin-type test method when $e/D \geq 3$ and $W/D \geq 4$.

4.5. Effect of fibre orientation

The fibre orientation in the laminate affects both the bearing strength and the mechanism of failure. The results show that the bearing strength obtained from the longitudinal test direction, is greater than for the LT test direction. This implies that the fibres contribute more to the bearing performance. For the GLARE 3 laminates with a cross-ply configuration (50% of fibres in 0° orientation and 50% in 90° orientation in each prepreg layer) we only acquired one bearing strength, for the direction parallel to the metal rolling direction.

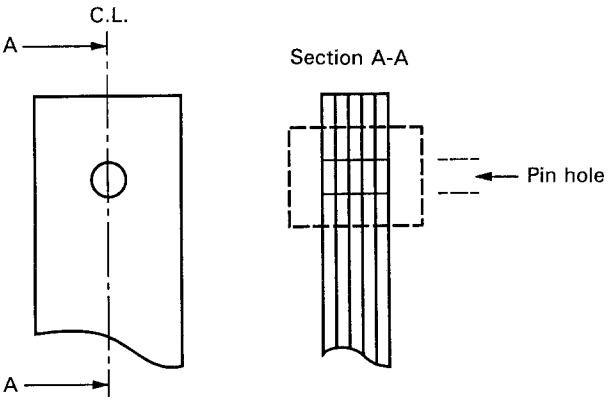

Figure 15 Cross-section through fibre–metal laminate bearing specimen centre for failure mode observation.

4.6. Bearing strength prediction

A rule-of-mixtures (ROM) approach can be applied to the prediction of fibre–metal laminate bolt-type bearing ultimate strength. This has been proved elsewhere [32] for an edge distance ratio $e/D = 2$. In the ROM, we assume that bearing failure occurs in the laminate when the individual layers (prepreg and aluminium) collapse simultaneously. This is because the separate layer stiffnesses will not play any significant role. This simple analysis is based on the aluminium volume

TABLE V Comparison between longitudinal bearing ultimate strengths (BUS) obtained by bolt-type bearing tests and rule-of-mixtures predictions for GLARE 2 and GLARE 3 laminates [32]

Lay-up (aluminium layer thickness, mm)	Aluminium volume fraction (%)	BUS (MPa) Test	Theory	Difference (%)
GLARE 2[a]				
3/2 (0.5)	75.00	767	762	− 0.7
4/3 (0.4)	68.09	714	707	− 1.0
5/4 (0.4)	66.67	689	696	+ 1.0
5/4 (0.3)	60.00	639	643	+ 0.6
3/2 (0.3)	64.29	709	677	− 4.5
GLARE 3[b]				
3/2 (0.3)	64.29	789	726	− 8.0
2/1 (0.2)	61.54	810	709	− 12.5
2/1 (0.3)	70.59	856	768	− 10.3
3/2 (0.2)	54.55	702	663	− 5.6
4/3 (0.4)	68.09	778	751	− 3.5
4/3 (0.5)	72.73	832	781	− 6.1
5/4 (0.4)	66.67	769	742	− 3.5

[a] $\sigma_{BUS}^{Al} = 959$ MPa for 2024-T3 aluminium alloy sheet bearing ultimate strength; $\sigma_{BUS}^{p} = 170$ MPa for unidirectional cured glass prepreg bearing ultimate strength.
[b] $\sigma_{BUS}^{Al} = 959$ MPa for 2024-T3 aluminium alloy sheet bearing ultimate strength; $\sigma_{BUS}^{p} = 308$ MPa for cross-ply cured glass prepreg bearing ultimate strength.

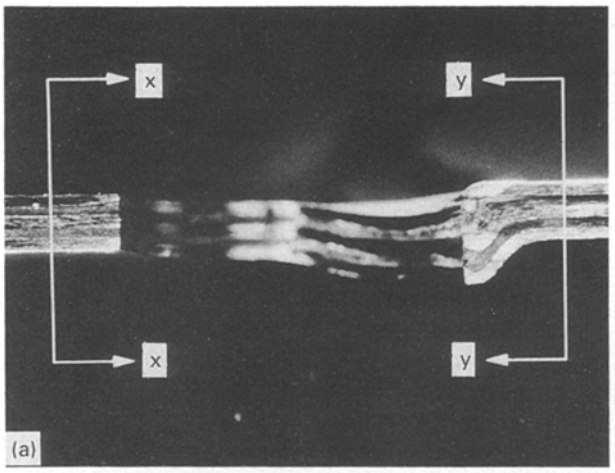

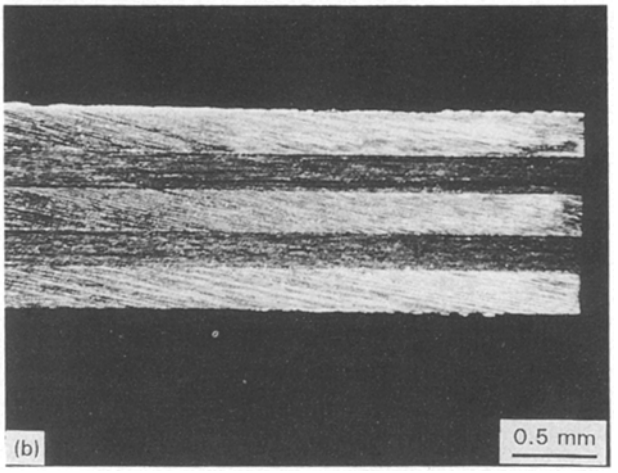

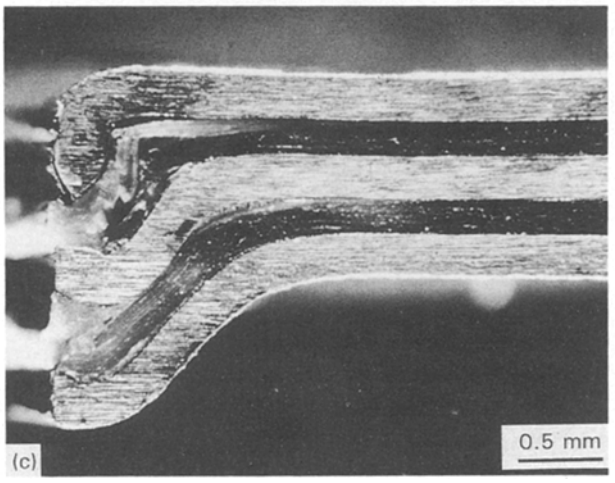

Figure 16 (a) Delamination buckling of bearing failure of 3/2 GLARE 2 laminate tested in the longitudinal direction with no lateral constraint (ASTM E-238); bearing load = 7478 N, bearing strength = 688 MPa, $e/D = 3$ and $W/D = 6$ ($D = 8$ mm). (b) Undeformed portion, view x–x; (c) deformed portion, view y–y.

fraction of the laminate:

$$\sigma_{ult}^{Lam} = \sigma_{ult}^{Al} V_f^{Al} + \sigma_{ult}^{p}(1 - V_f^{Al}) \quad (7)$$

where σ_{ult}^{Lam} is the laminate bearing ultimate strength, σ_{ult}^{Al} the aluminium alloy bearing ultimate strength, σ_{ult}^{p} the cured fibre–epoxy bearing ultimate strength and V_f^{Al} the aluminium alloy volume fraction.

The results are presented in Table V. They demonstrate that a good prediction of bearing ultimate strength of GLARE 2 laminates was achieved. The relatively lower calculated stresses for GLARE 3 laminates are probably due to the beneficial contribution of cross-ply fibres in the overall laminate sandwich.

4.7. Observation of bearing failure modes

Observations of failure modes of the tested GLARE 2 laminate bearing specimens in both the longitudinal and LT directions obtained from pin-type (unconstrained) and bolt-type (constrained) testing procedures were examined using optical microscopy. Photomicrographs were taken from above and below the pin hole along section A–A as illustrated in Fig. 15. Fig. 16 and 17 show bearing failure patterns of GLARE 2 laminates in the longitudinal direction for

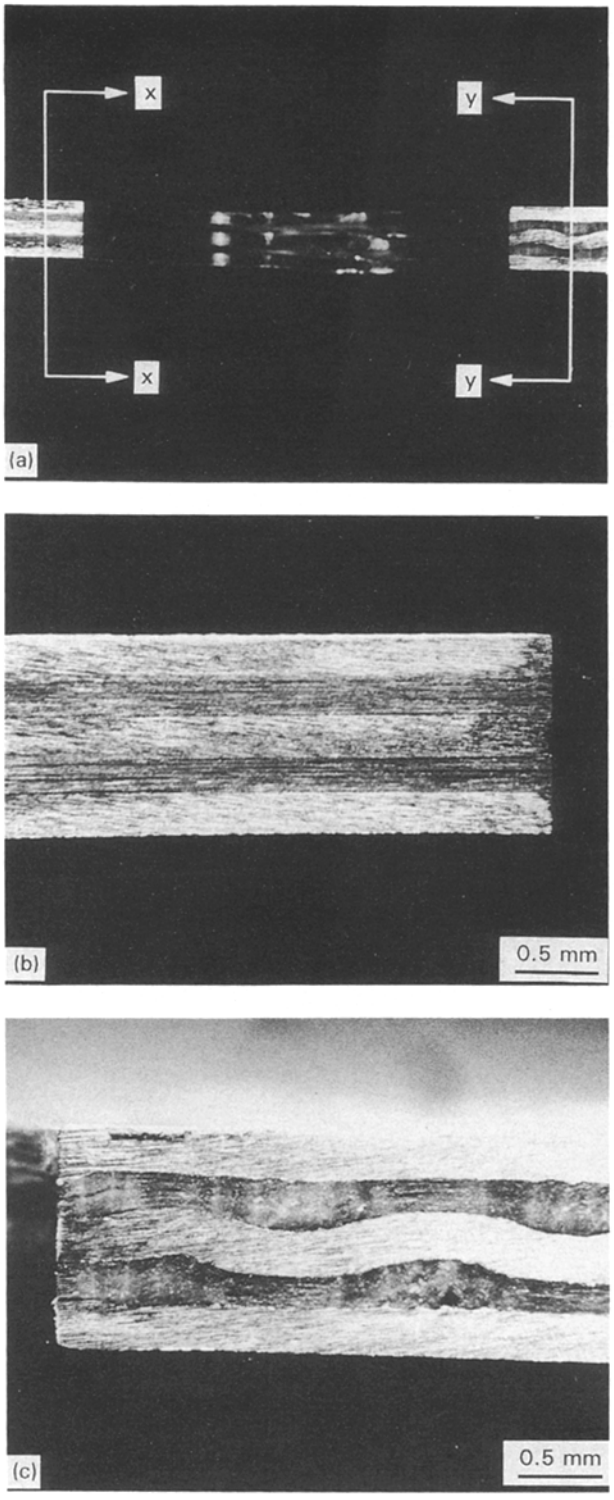

Figure 17 (a) Delamination buckling free of bearing failure of 3/2 GLARE 2 laminate tested in the longitudinal direction with lateral constraint (ASTM D-953); bearing load = 10 887 N, bearing strength = 977 MPa, $e/D = 3$ and $W/D = 6$ ($D = 8$ mm). (b) Undeformed portion, view x–x; (c) deformed portion, view y–y.

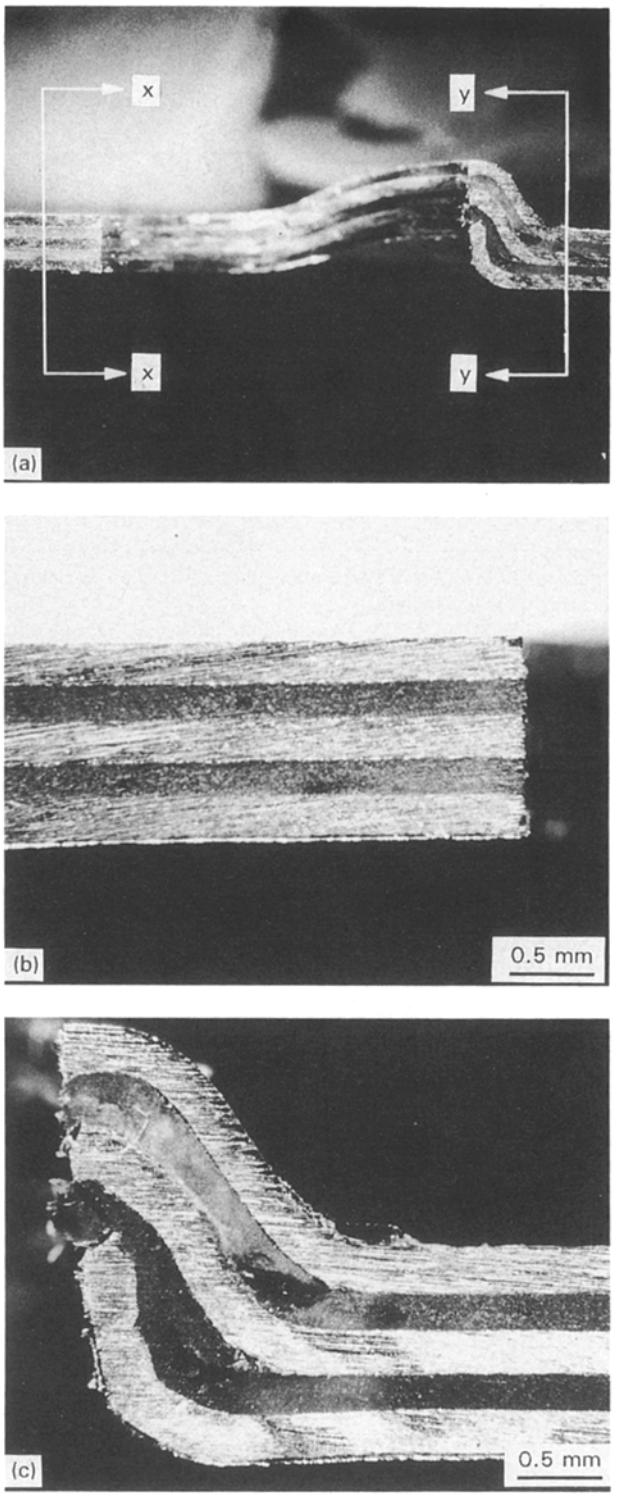

Figure 18 (a) Delamination buckling of bearing failure of 3/2 GLARE 2 laminate tested in the long-transverse direction with no lateral constraint (ASTM E-238); bearing load = 6137 N, bearing strength = 548 MPa, $e/D = 3$ and $W/D = 6$ ($D = 8$ mm). (b) Undeformed portion, view x–x; (c) deformed portion, view y–y.

both testing procedures. Bearing failure patterns of GLARE 2 laminates in the LT direction for both testing procedures are shown in Figs 18 and 19. The figures indicate that a delamination buckling bearing failure has been observed in the testing procedure which has no side constraint (ASTM E-238); however, no visual evidence of macrodelamination buckling bearing failure was found using the testing procedure of ASTM D-953 (with lateral constraint). Because no delamination buckling occurs in the latter testing procedure, an increased bearing ultimate strength over pin-load specimen values is to be expected. Another interesting finding is that the wavy deformation (in-phase mode of buckling) found in the centre layer of aluminium alloy of the laminate in the longitudinal direction is due to the alloy layer being compressed from both sides by fibre prepregs. A similar phenomenon is also seen in GLARE 3 laminates as shown in

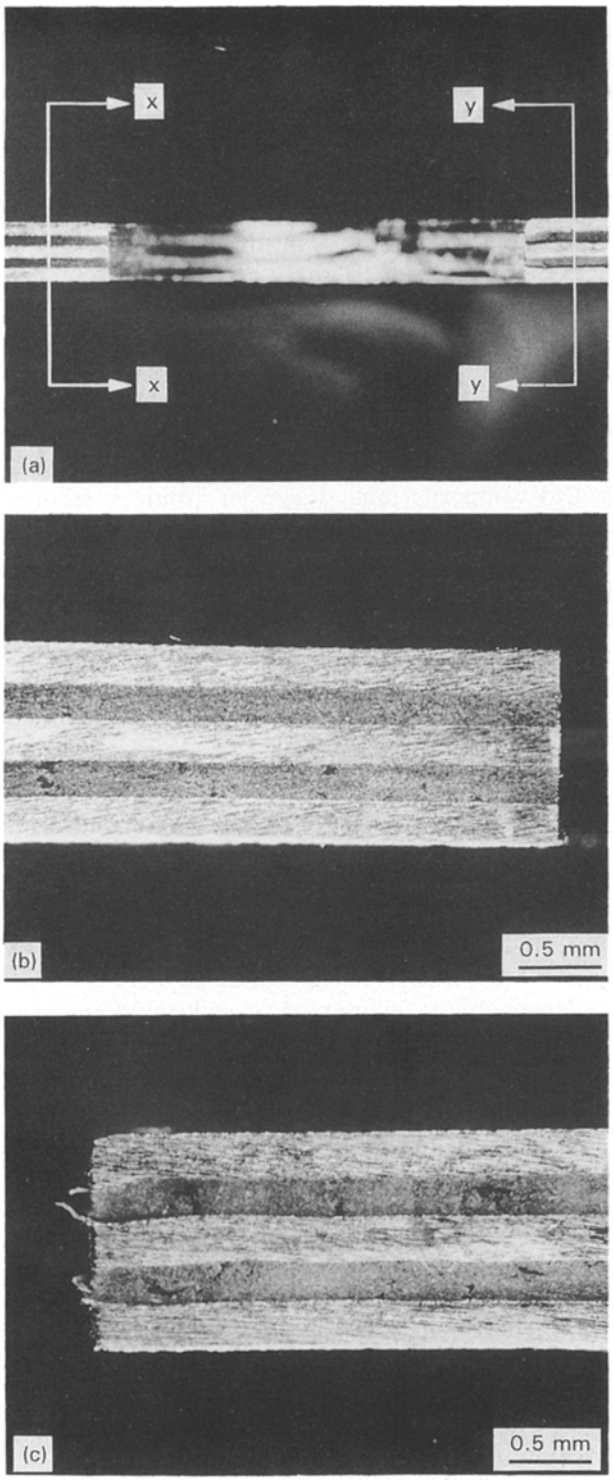

Figure 19 (a) Delamination buckling free of bearing failure of 3/2 GLARE 2 laminates tested in the long-transverse direction with lateral constraint (ASTM D-953); bearing load = 10 742 N, bearing strength = 959 MPa, $e/D = 3$ and $W/D = 6$ ($D = 8$ mm). (b) Undeformed portion, view x–x; (c) deformed portion, view y–y.

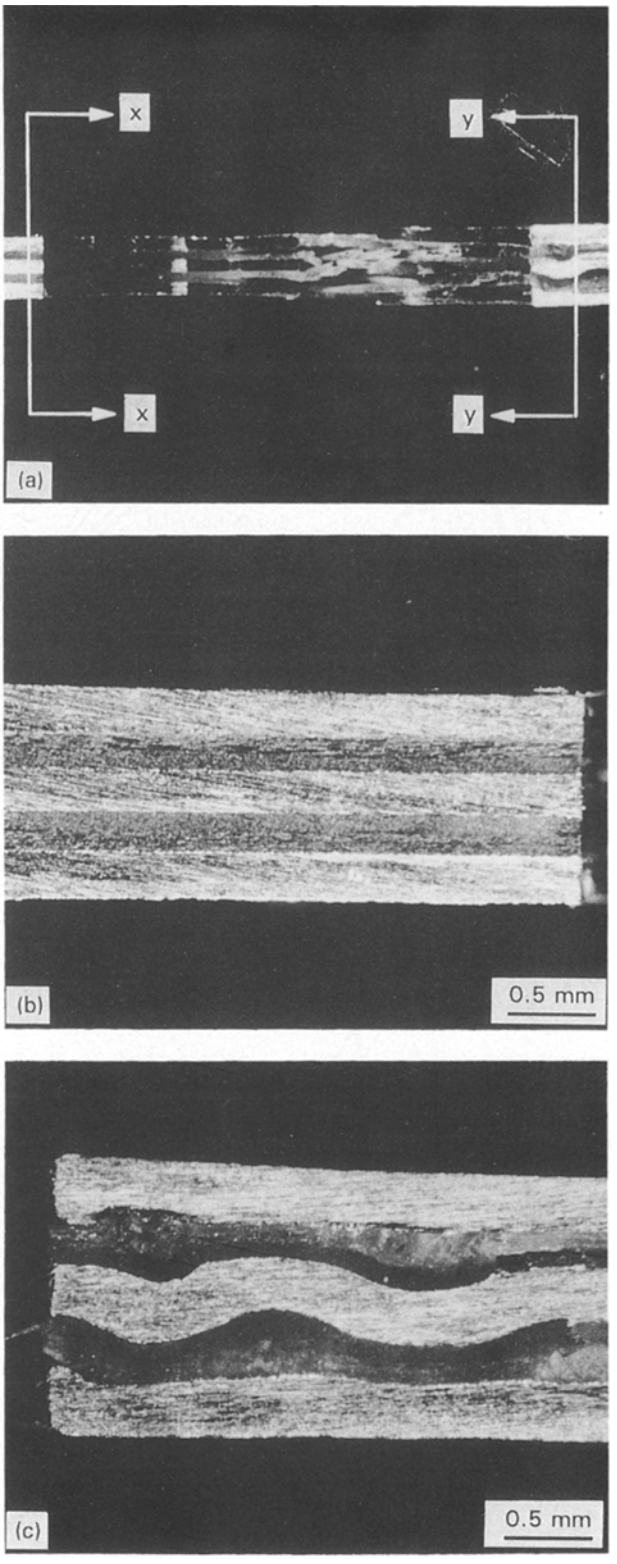

Figure 20 (a) Delamination buckling free of bearing failure of 3/2 GLARE 3 laminates tested in the longitudinal direction with lateral constraints (ASTM D-953); bearing load = 11 422 N, bearing strength = 1017 MPa, $e/D = 3$ and $W/D = 6$ ($D = 8$ mm). (b) Undeformed portion, view x–x; (c) deformed portion, view y–y.

Fig. 20. However, in this aluminium alloy wavy deformation is not found in the LT bearing specimens. This wavy deformation of the centre layer of aluminium alloy sheet introduces a great interest for future research of bearing failure mode analysis.

4.8. Joint structural efficiency

Joint structural efficiency is defined as a computed ratio of joint strength to laminate tensile strength. Diagrams of joint efficiency are used for structural fastened joint design for aerospace applications. Hart-Smith [35] has investigated the relationship between the strengths of bolted joints in ductile, fibrous composites, and brittle materials. Based on the bearing strength data obtained from the effect of pin hole diameter-to-width ratio, the joint structural efficiency

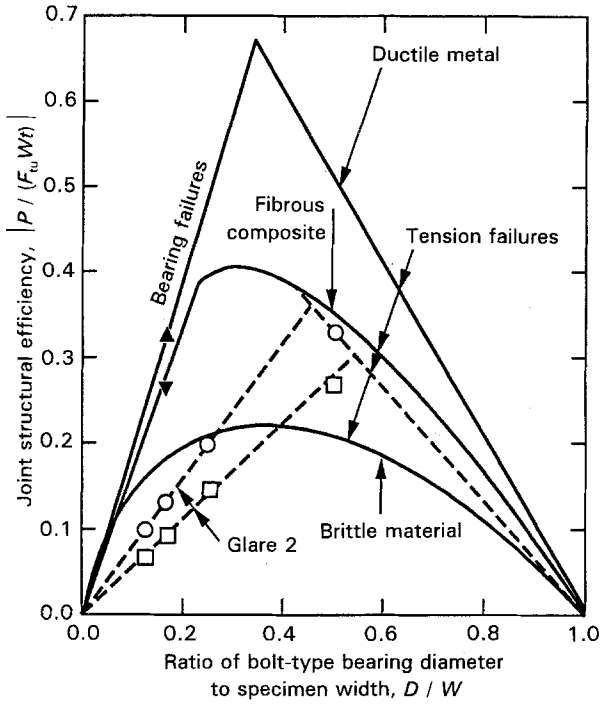

Figure 21 (——) Relations between strengths of bolted joints in ductile, fibrous composites and brittle materials [35], compared with data for alloy 2024-T3 and longitudinal 3/2 GLARE 2 laminate. 2024-T3: (▼) $e/D = 1.5$, (▲) $e/D = 2.0$. GLARE 2: (○) ASTM D-953, (□) ASTM E-238.

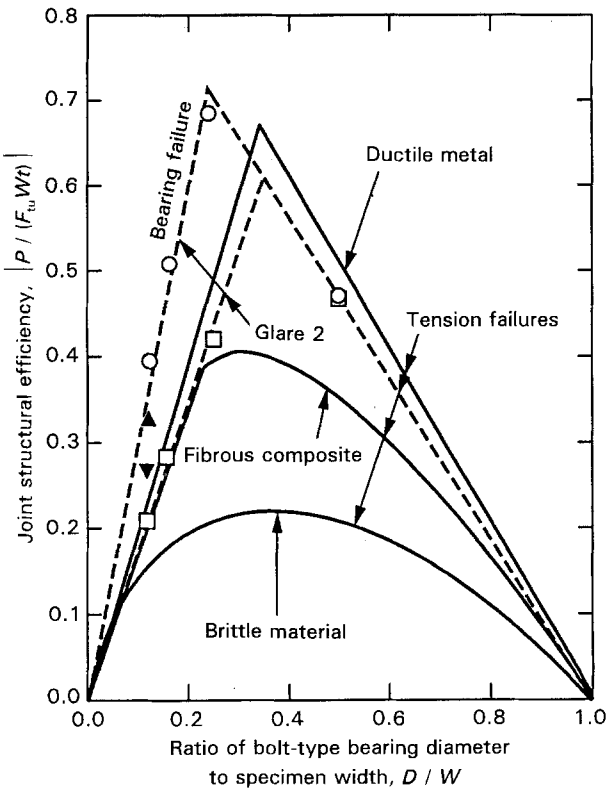

Figure 22 (——) Relations between strengths of bolted joints in ductile, fibrous composites and brittle materials [35] compared with data for alloy 2024-T3 and long-transverse 3/2 GLARE 2 laminate. 2024-T3: (▼) $e/D = 1.5$, (▲) $e/D = 2.0$. GLARE 2: (○) ASTM D-953, (□) ASTM E-238.

diagrams of GLARE laminates in both the longitudinal and LT directions have been established, as shown in Figs 21 and 22. The lines for GLARE 2 laminates were derived purely on the basis of test results. There are bearing failures in the left region of the picture (when $W/D \geq 4$) where the bearing specimen width is large in comparison with the hole diameter. As the pin hole is moved closer to the side edge of the specimen (or the specimen is narrowed), there is a change in failure mode to tension-through-the-hole (when $W/D \leq 2$).

In Figs 21 and 22 the peak strength occurs either at a geometry associated with the tension failure mode or at an abrupt transition between bearing and tension failures; in either case peak strength is associated with a definite W/D value, which is projected to a value of 4 for LT-orientation GLARE 2 and a value of 2 for longitudinal-orientation GLARE 2 laminates in the bolt-type test procedure. Any effort to impose on a bolted composite joint design an arbitrary requirement of failure by bearing only (by using a sufficiently large value of W/D) to ensure a less catastrophic failure mode must necessarily be associated with a significant reduction in joint strength and, hence, in structural efficiency. In addition, the results from Figs 21 and 22 show that joint structural efficiencies in both the longitudinal and LT directions have a trend compatible with those for fibrous composites and ductile material.

5. Conclusions

From this study, several conclusions can be drawn as follows:

1. Fibre–metal laminate bearing strength is shown to depend on the failure mode as influenced by specimen geometry and test method.
2. A bearing test fixture with lateral (bolt-type) constraint produces a more representative structural failure mode than does the unconstrained pin-type test.
3. A bolt-type test fixture (modified ASTM D-953) gives a bearing strength at least 20% higher than that given by a pin-type test fixture (ASTM E-238) when the full bearing strength is being developed.
4. A minimum edge distance ratio e/D of 3 and width radio W/D of 4 should be used to develop the full bearing strength for fibre–metal laminates.
5. A D/W value of about 0.25 for long-transverse orientation or 0.45 for longitudinal orientation of the specimen provides optimum structural joint efficiency when the bolt-type (ASTM D-953) bearing test procedure is employed. The joint structural efficiency of LT-orientation GLARE 2 laminates has been shown to be comparable with that of aluminium alloy sheets.
6. A rule-of-mixtures approach can be applied to the prediction of bolt-type bearing ultimate strength in fibre–metal laminates.

6. Recommendations

The detailed mechanism of wavy deformation of the centre layer of aluminium alloy sheet in the longitudinal bearing test specimen should be further studied. The failure mechanism can be correlated with its monotonic bearing behaviour which is exhibited in the load versus displacement curve. Bearing properties

for both cured prepregs and pure aluminium alloy sheets should be determined, based on the geometry effect with the support of rule-of-mixtures predictions.

Acknowledgements

The authors are grateful to the Structural Laminates Co. for the provision of materials and research support. In addition, they wish to acknowledge Mr M. Hakker and Mr J. Mensink of Delft University for performing all the bearing tests and Mr J. C. Vilsack of Alcoa Technical Center for providing photomicrographs of failure modes study.

References

1. R. MARISSEN and L. B. VOGELESANG, in Proceedings of International SAMPE Conference, Cannes, France, 1981.
2. L. B. VOGELESANG, R. MARISSEN and J. SCHIJVE, in Proceedings of 11th ICAF Symposium, Noordwijkerhout, The Netherlands, 1981.
3. J. W. GUNNINK, L. B. VOGELESANG and J. SCHIJVE, in Proceedings of 13th Congress of the International Council of Aerospace Science, Seattle, Washington, 1982, p. 990.
4. L. B. VOGELESANG and J. W. GUNNINK, "ARALL, A Material for the Next Generation of Aircraft. A state-of-the Art," Report LR-400 (Department of Aerospace Engineering, Delft University of Technology, The Netherlands, 1983).
5. J. W. GUNNINK, M. L. C. E. VERBRUGGEN and L. B. VOGELESANG, *Vertica* **10** (1986) 241.
6. L. B. VOGELESANG and J. W. GUNNINK, *Mater. Design* **7** (2) 1986.
7. R. J. BUCCI, L. N. MUELLER, R. W. SCHULTZ and J. L. PROHASKA, in Proceedings of 32nd International SAMPE Symposium and Exhibition, Anaheim, California, 1987, p. 902.
8. Proceedings of ARALL Laminates Technical Conference, Champion, Pennsylvania (Alcoa Laboratories, Alcoa Center, Pennsylvania, 1987).
9. R. J. BUCCI, L. N. MUELLER, L. B. VOGELESANG and J. W. GUNNINK, in "Aluminum Alloys–Contemporary Research and Applications", Treatise on Materials Science and Technology Vol. 31 (Academic, San Diego, CA, 1989) p. 295.
10. J. W. GUNNINK and L. B. VOGELESANG, in Proceedings of 35th International SAMPE Symposium and Exhibition, Anaheim, California, 1990, p. 1708.
11. *Idem*, in Proceedings of 36th International SAMPE Symposium and Exhibition, San Diego, California, 1991, p. 1509.
12. M. A. GREGORY, and G. H. J. J. ROEBROEKS, in Proceedings of 30th Annual Conference of Metallurgists (Metallurgical Society of CIM, Ottawa, 1991).
13. L. H. van VEGGEL, in Proceedings of 42nd Annual General Meeting of the Aeronautical Society of India, Calcutta, 1990.
14. W. LEODOLTER and R. G. PETTIT, Douglas Paper No. 8164, in Proceedings of Specialist Conference on ARALL Laminates, Delft University of Technology, The Netherlands, 1988.
15. R. G. PETTIT, in Proceedings of AEROMAT'91, Long Beach, CA, May 1991.
16. H. F. WU, *J. Mater. Sci.* **25** (1990) 1120.
17. H. F. WU and J. F. DALTON, in Proceedings of 36th International SAMPE Symposium and Exhibition, San Diego, California, 1991, p. 2040.
18. H. F. WU, *J. Mater. Sci.* **26** (1991) 3721.
19. "Metallic Materials and Elements for Aerospace Vehicles Structures," Military Handbook MIL-HDBK-5F, Vols. 1 and 2 (US Department of Defense, 1990).
20. H. F. WU, R. J. BUCCI, R. H. WYGONIK and R. C. RICE, in Proceedings of AEROMAT' 91, Long Beach, California, May 1991 and ICCM/8, Honolulu, Hawaii, July 1991.
21. *Idem, AIAA J. Aircraft*, **30** (1993) 275.
22. E. W. GODWIN and F. L. MATTHEWS, *Composites* (1980) 155.
23. T. A. COLLINGS, in "Joining Fibre-Reinforced Plastics" (Elsevier Applied Science, London, 1987).
24. F. L. MATTHEWS, *ibid.*
25. G. KRETSIS and F. L. MATTHEWS, *Composites* (1985) 92.
26. T. A. COLLINGS, *ibid.* (1982) 241.
27. J. H. STOCKDALE and F. L. MATTHEWS, *ibid.* (1976) 34.
28. I. ERIKSSON, *J. Compos. Mater.* **24** (1990) 1246.
29. D. F. ADAMS, *Polym. Compos.* **11** (1990) 286.
30. W. R. BROUGHTON, M. KUMOSA and P. HULL, *Compos. Sci. Technol.* **38** (1990) 299.
31. ASTM E-238, "Standard Test Method for Pin-Type Bearing Test of Metallic Materials" (1984).
32. W. J. SLAGTER, *J. Compos. Mater.* **26** (1992) 2542.
33. H. F. WU, "Parametric Studies of Bearing Strength for Fiber/Metal Laminates," SLC Report SL-019-C (Structural Laminates Co., New Kensington, PA, 1991).
34. ASTM D-953, "Standard Test Method for Bearing Strength of Plastic Properties" (1987).
35. L. J. HART-SMITH, Douglas Aircraft Co. Paper DP 6748A (1978), also contained in "Fibrous Composites in Structural Design", edited by E. M. Lenoe, D. W. Oplinger and J. J. Burke (Plenum, New York, 1980) p. 543.

Received 25 March
and accepted 17 December 1993